Supplementary Material (ESI) for Lab on a Chip

Tunable Liquid Gradient Refractive Index (L-GRIN) Lens with Two Degrees of Freedom

Xiaole Mao,[ab] Sz-Chin Steven Lin,[a] Michael Ian Lapsley,[a] Jinjie Shi,[a] Bala Krishna Juluri[a] and Tony Jun Huang*[ab]

[a] *Department of Engineering Science and Mechanics, The Pennsylvania State University, University Park, PA 16802, USA. Fax: 814-865-9974; Tel: 814-863-4209; E-mail: junhuang@psu.edu*
[b] *Department of Bioengineering, The Pennsylvania State University, University Park, PA 16802, USA.*

Device Fabrication and Experiment Setup

The photomask was designed using AutoCAD software (http://usa.autodesk.com/) and converted to GDSII format using a format-conversion package, LinkCAD-5 (http://www.linkcad.com). It was then printed using a high-resolution laser writer, DWL66 (Heidelberg Instruments, http://www.himt.de). The polydimethylsiloxane (PDMS) microchannels were fabricated using standard soft lithography technique. The mold for the PDMS was fabricated on a silicon wafer (TechGophers, Chino Hills, CA) by Deep Reactive Ion Etching (DRIE, Adixen, Hingham, MA). The positive photoresist SPR-220-7 (MicroChem, Newton, MA) was lithographically patterned onto the silicon wafer with an etch depth of 155 μm (the same as the diameter of the optical fiber) to act as a mask for DRIE. The final mold depth was confirmed using a profilometer (KLA-Tencor, San Jose, CA). The silicon mold was silanized by exposure to 1H,1H,2H,2H-perfluorooctyl-trichlorosilane (Sigma Aldrich, St. Louis, MO) vapor inside a vacuum chamber, in order to reduce surface energy and hence the damage to the PDMS channel caused during the demolding process. This step increased the smoothness of the PDMS

sidewall and reduced scattering loss during the focusing process. The Sylgard^{TM} 184 silicone elastomer base and curing agent (Dow Corning, Midland, MI) were mixed at a 10:1 weight ratio, cast onto the silicon mold, and stored in a -20 ºC freezer overnight to allow bubbles trapped on the silicon mold to migrate to the surface or dissolve. The PDMS was then cured at 70 ºC for one hour and peeled off from the mold. Inlets and outlets were created with a silicon carbide drill bit before the PDMS substrate was bonded to a glass slide. The inlets and outlets of the device were connected to syringe pumps (KDS 210, KD scientific, Holliston, MA) using polyethylene tubes (Becton Dickson, Franklin Lakes, NJ).

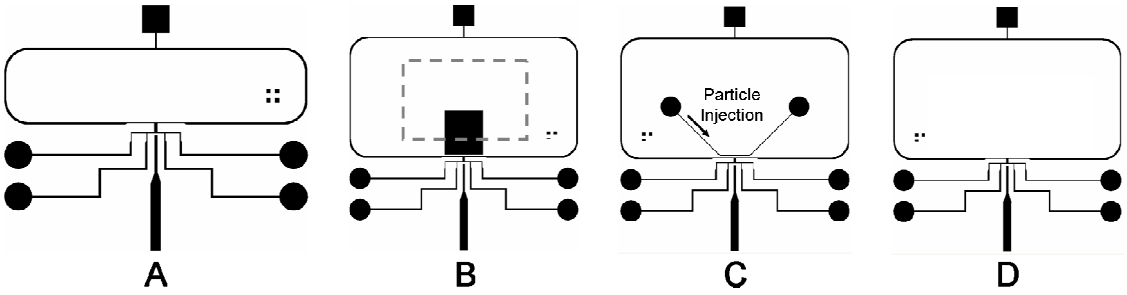

Fig. S1 Photomasks of the devices used for (A) translation mode ray tracing experiments (main channel length = 400 μm, Fig. 3 in the main text), (B) focused beam profile characterization (main channel length = 250 μm, Fig. 4A in the main text), and (C) flow cytometry test (main channel length = 250 μm, Fig. 5 in the main text), and (D) swing mode ray tracing experiments (main channel length = 250 μm, Fig. 6 in the main text)

Four different device designs (Fig. S1) were used in the experiments for different characterization purposes. These devices shared similar fluidic components except for the main channel length. In the long-version L-GRIN device (Fig. S1A), the main channel was made 400 μm long in order to cover a larger focal distance range in the translation-

mode ray-tracing experiment (Fig. 3 in the main text). The rest of designs were based on the short-version devices (main channel length = 250 μm). The second design (Fig. S1B) was used in side-view imaging experiments to characterize the focused beam profile (Fig. 4A in the main text). A patch was placed near the L-GRIN main channel (100 μm gap). The patch and PDMS substrate were cut along the dotted line to create an optical window, which allowed the focused light to exit the L-GRIN lens. A 2 mm x 2 mm 90-degree prism (Edmund Optics, Barrington, NJ) was placed near the optical window to deflect light into the microscope lens so that the focusing pattern parallel to the substrate could be directly visualized using an upright microscope (Fig. S2). The third design (Fig. S1C) was used in the flow cytometry test (Fig. 5 in the main text). The fourth design (Fig. S1D) was used in the swing-mode ray-tracing experiment (Fig. 6 in the main text).

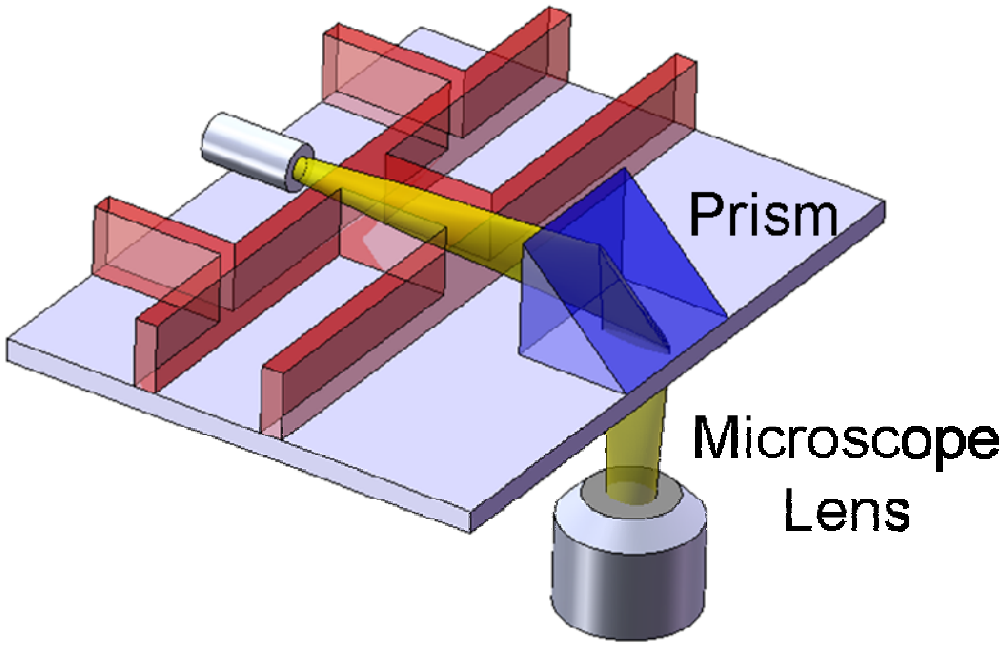

Fig. S2 Schematic of the side-view imaging setup for characterizing the focused light beam profile in Fig. 4A in main text.

The Dependence of Focal Length and Swing Angle on Sheath Flow Rate

The focal distance, defined as the distance between the focusing position and the aperture of the optical fiber, was measured from the simulation and experimental results (Fig. 2 and Fig. 3) and plotted as a function of the sheath flow rate (Fig. S3). A good agreement between the simulation and experiment was found. The tuning range for the focal distance is approximately 1,200 to 500 μm as the sheath flow rate increases. It is possible to achieve shorter focal distance, and hence the larger NA, by increasing the refractive index contrast (i.e., increasing the concentration of CaCl2 solution or adapting other fluids with higher refractive index).

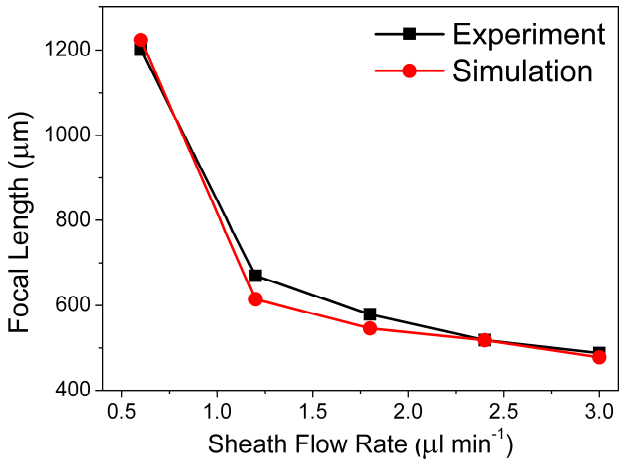

Fig. S3 Focal length of the L-GRIN lens as a function of sheath flow rate. The data were measured from the ray-tracing simulation and experiments in Fig. 2 and Fig. 3 in the main text, respectively. A good agreement between the simulation and experiment was found. (Fig. 2 and Fig. 3 in main text did not show the focal point for sheath flow rate = 0.6 μl min^{-1}. The focal length for flow rate = 0.6 μl min^{-1} were estimated from extrapolation).

The swing angle for each flow rate was measured from the simulation and experimental results in Fig. 6 and Fig. 7 and plotted as a function of the sheath flow rate (Fig. S4). A good agreement between the simulation and experiment was found. The

results show a maximum swing angle of approximately ± 12°. A larger swing angle is possible by further optimizing the refractive index gradient and channel geometries.

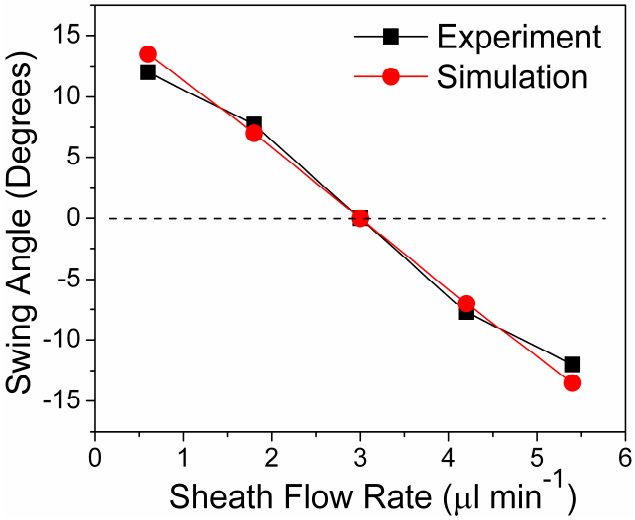

Fig. S4 Swing angle of the L-GRIN lens as a function of the sheath flow rate. The data were measured from the ray-tracing simulation and experiments in Fig. 6 and Fig. 7 in the main text, respectively. A good agreement between the simulation and experiment was found.

Caption of Video S1 and S2

Video S1 (Video of Fig. 3):

The video shows the ray-tracing characterization of the L-GRIN lens in the translation mode. Dynamic changes of the focal length and flow patterns are more evident in this video than in Fig. 3.

Video S2 (Video of Fig. 6):

The video shows the ray-tracing characterization of the L-GRIN lens in the swing mode. Dynamic changes of the output light direction and the shift of optical axis due to the variable flow injection are more evident in this video than in Fig. 6.